April 2012

Characterization of Senescence Regulation by Smurf2 and Notch3 in vitro and in vivo

Laura Catherine Wong
Worcester Polytechnic Institute

MQP-BIO-JBD-0011

Characterization of Senescence Regulation by Smurf2 and Notch3 *in vitro* and *in vivo*

A Major Qualifying Project Report

Submitted to the Faculty of the

WORCESTER POLYTECHNIC INSTITUTE

in partial fulfillment of the requirements for the

Degree of Bachelor of Science

in

Biology and Biotechnology

by

_____
Laura Fineman

April 26, 2012

APPROVED:

_____
Hong Zhang, Ph.D.
Cell Biology
UMass Medical School
Major Advisor

_____
Joseph B. Duffy, Ph.D.
Biology and Biotechnology
WPI Project Advisor

ABSTRACT

One of the main functions of a tumor suppressor is to repress cell division, sometimes by inducing cellular senescence. Smurf2 and Notch3 have previously been identified in our laboratory as tumor suppressors *in vitro*. It is not well understood how these genes regulate senescence. The purpose of this project is to better understand the mechanisms underlying the functions of these genes in senescence. A genetic screen using short hairpin RNAs (shRNAs) was carried out to identify genes downstream of Smurf2 or Notch3 in the senescence pathways. Five candidate genes were further analyzed in fibroblasts. To characterize the function of Smurf2 in senescence *in vivo*, a Cre-LoxP system was used to study the consequence of Smurf2 overexpression in mice. I found that Smurf2 impacts growth and regulates p21 in young mice.

ACKNOWLEDGEMENTS

I would like to thank Professor Hong Zhang for giving me the opportunity to join his lab, and for his support and guidance throughout the experimental and writing process. I would like to thank Hang Cui for donating her time in helping me become proficient at the techniques and assays necessary for the completion of this project. I would also like to thank Yahui Kong, Charusheila Ramkumar, and Ivan Lebedev for teaching me additional skills that were useful for my project. Finally, I would like to thank Professor Joseph Duffy for his guidance in choosing a good lab to work in, his assistance with MQP editing, and his support as my academic advisor for the past four years.

TABLE OF CONTENTS

BACKGROUND

Replicative Senescence

Normal cells, including fibroblast cells, in culture replicate a finite number of times before entering senescence (Hayflick and Moorhead, 1961). When entering senescence, cells are permanently arrested in the G1 phase of the cell cycle, meaning they do not enter the replicative S phase (Sherwood et al., 1988). This is not to be confused with quiescent cells, which are temporarily arrested in the G0 phase due to a high cell density (Zhang, 2007). Senescent cells have a distinct morphology; they usually are larger than young cells (Bayreuther et al., 1988). Senescent cells also express an acidic beta-galatosidase. When stained at a pH of 6, this enzyme produces a blue coloring that becomes detectable after about 16 hours (Dimri et al., 1995)

Telomere Shortening

Telomeres are structures at the ends of chromosomes that function in chromosomal protection (Kim et al., 1994). The enzyme telomerase is a way of maintenance of these chromosomal ends; however, it is only found in immortal cancer cells (Kim et al., 1994). The majority of somatic cells do not express this enzyme (Kim et al., 1994). As these somatic cells divide, the amount of telomeric DNA decreases; this loss and eventual deletion of necessary sequences in the genome contributes to the finite replication observed (Harley et al., 1990).

Senescence Pathways

Telomere shortening, or DNA damage and cell stress are the two big reasons why cells will senesce. Each signal induces a parallel pathway: it is found that DNA damage induces the p53-p21 pathway (Herbig et al., 2004) and cell stress induces the p16-RB pathway (Benanti and Galloway, 2004).

p53-p21 Pathway

ATM (ataxia-telangiectasia mutated) and ATR (Rad3-related) are primary PI3K-like protein kinases in the DNA damage pathway (Herbig et al., 2004). ATM responds to double-strand breaks and ATR is a primary mediator in ultraviolet light damage and stalled replication forks (Herbig et al., 2004). These kinases have been shown to phosphorylate and activate p53, which induces replicative senescence (Herbig et al., 2004).

p53 affects cellular replication by it's ability to bind to DNA; increased binding ability leads to replicative senescence (Vaziri et al., 1997). Disruption of the p53 protein has been shown to extend proliferation of human fibroblast cells and p53 levels are shown increase in aging fibroblast cells (Vaziri et al., 1997). The increase of p53 is due to its phosphorylation by ATM and ATR following DNA damage from shrinking telomeres (Vaziri et al., 1997). Increased p53 binding increases the transcription of the p21 gene, a cell cycle regulator whose expression has been seen to increase in senescing cells (Herbig et al., 2003).

p16-Rb Pathway

Although telomere erosion is a main part of the replicative senescence model, other factors also contribute to the senescent phenotype (Hütter et al., 2002). Oxidative damage is a major cause of aging as well; the oncogene RAS is activated after oxidative damage occurs and can induce premature senescence (Hütter et al., 2002).

Activated RAS up-regulates the cyclin-dependent kinase inhibitor p16 (Benanti and Galloway, 2004), whose expression is independent of telomere degradation and p53 expression (Herbig et al., 2004). p53 is able to inhibit cyclin-dependent kinase (CDK)4 and CDK6, who inactivate Rb (retinoblastoma) (Ruas and Peters, 1998). So increased levels of p16 lead to increased levels of Rb (Ruas, 1998). However, Rb-induced senescence is not completely p16 dependent; p21 has been shown to up-regulate Rb in the same way as p16 (Beauséjour et al., 2003). Rb activation induces senescence by repression of E2F-dependent promoters, leading to G_1 cell cycle arrest (Benanti et al., 2004).

Notch Signaling

The Notch signaling pathway is not fully understood, but it consists of the Notch receptors, ligands, modifiers, and transcription factors (Allenspach et al., 2002). Notch3 is one of four mammalian Notch receptors; it differs from Notch4 in that it contains cytokine response (NCR) regions and differs from Notch1 and Notch2 in that it lacks C-terminal transcriptional activation domains (TAD) (Allenspach et al., 2002).

Notch Signaling Pathway

Notch signaling starts with binding to the ligand; this releases the active intracellular domain of Notch (ICN) into the cytoplasm (Allenspach et al., 2002). From the cytoplasm, it relocates to the nucleus, where it induces transcription of several basic-helix-loop-helix-orange proteins that repress gene expression (Allenspach et al., 2002). One of the major players in transcriptional activation is the Mastermind-like (MAML) protein; it aids in the stabilization of the DNA-binding complex that includes ICN (Oyama et al., 2007).

Notch3 and Pathways

It has been shown that Notch3 depletion of the cell decreased the levels of p21; this was consistent with the decreased levels of the ICN target, HES1 (Giovannini et al., 2009). HES1 increase has been previously linked with up-regulation of p21 (Giovannini et al., 2009).

Smurf2 Regulates Senescence

Smurf2, or SMAD specific E3 ubiquitin protein ligase, encodes a 748 amino acid human protein that is responsible for ubiquitinating Smad2, which leads to its degradation; Smads are important regulators for TGF-β (transforming growth factor-beta) (Lin et al., 2000).

Smurf2 and Senescence

Microarray analysis from our lab has shown that telomere shortening increases Smurf2 levels; furthermore, overexpression of the gene is also sufficient to induce replicative senescence (Zhang and Cohen, 2004). Two forms of this protein are used in this project: the above-mentioned wild type form and a cystine to alanine mutation at position 716 in the HECT domain of the protein (Lin et al., 2000). Although the C716A mutant is unable to ubiquitinate Smad2, it still operates under a similar mechanism to the wild type (Zhang et al., 2008).

Smurf2 in the Pathway

Smurf2 has been shown to affect both the p53/p21 and the p16/Rb pathways; however, it requires at least one of the pathways to be functional in order to induce senescence (Zhang and Cohen, 2004). Smurf2 enters the pathway at either p21 or p16 (Figure 1). Increase in Smurf2 has been shown to correlate with increased expression of p21 (Zhang et al., 2008). Smurf2 does not directly interact with p16, Id1 (inhibitor of differentiation of DNA binding 1) acts as a mediator (Kong et al., 2011). Id1 represses p16 expression, so the ubiquitination and degradation of Id1 by Smurf2 allows p16 to be expressed and induce senescence (Zheng et al., 2004).

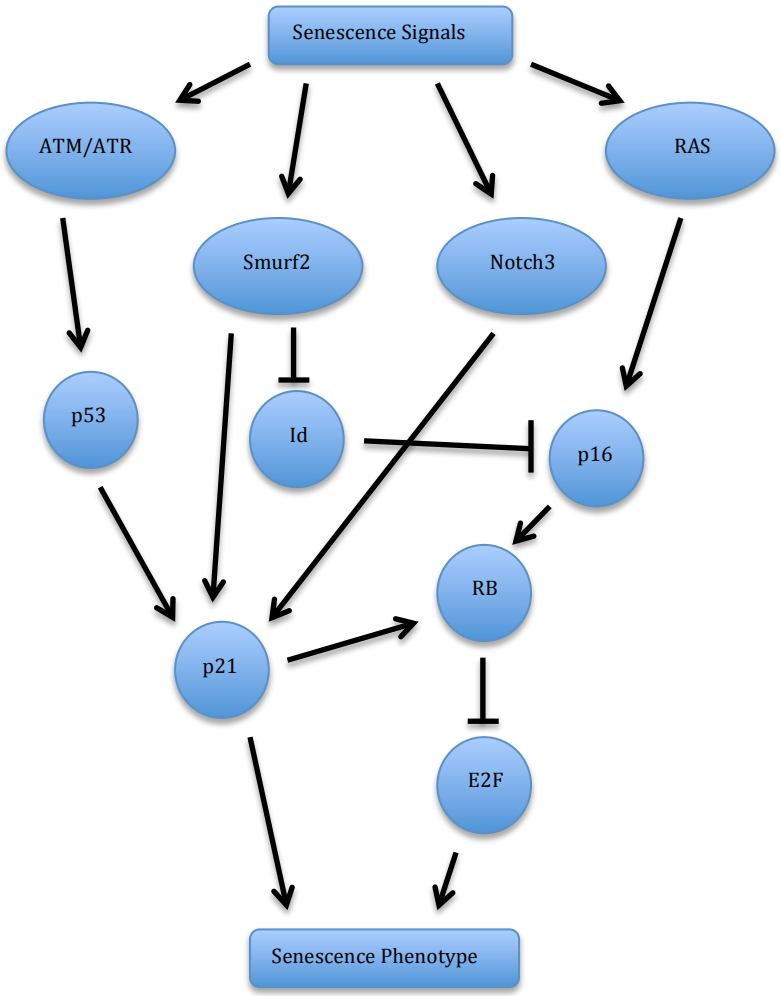

Figure 1: Notch3's and Smurf2's Interaction with the p53-p21 and the p16-RB Senescence Pathways. Notch3 is shown to up-regulate p21 levels. Smurf2 has been shown to both up-regulate p21 levels and up-regulate p16 levels through repression of Id.

Identification of Genes Downstream of Notch3 Using shRNA Screening

The *in vitro* part of this MQP consisted of determining what genes were downstream of Smurf2 and Notch3. Smurf2 screening previously done by our lab had already generated a group of clones that needed to be validated, so I concentrated on Notch3 screening. The idea was if a gene that was in fact downstream of either Smurf2 or Notch3 was knocked down, the senescence

pathway would be interrupted and fibroblast cells would be able to escape Smurf2 or Notch3-induced senescence.

The shRNA libraries used for the screening were the Expression Arrest pGIPZ Lenti-viral shRNAmir Library from Open Biosystems, as shown in Figure 2. The library was divided into pools, each pool containing 5,000 shRNAs. The lenti-viral vector is compromised of two complementary 22bp sequences that would pair into a hairpin sequence when translated into mRNA.

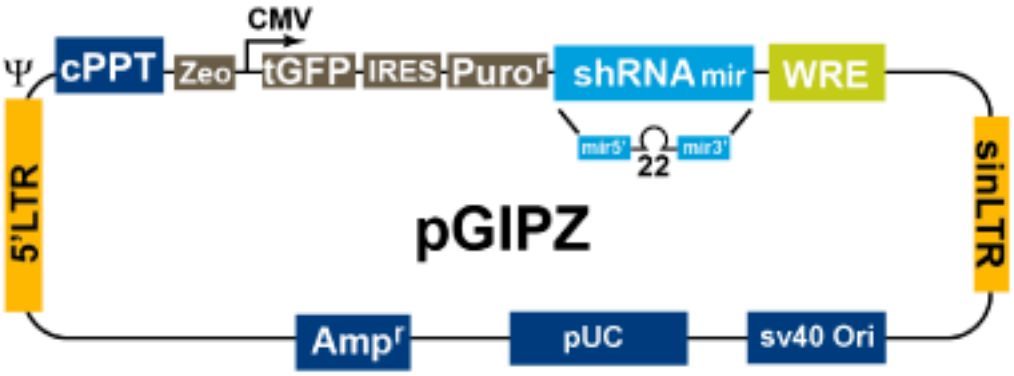

Figure 2: Design of the shRNAmir vector. The shRNAmir system incorporates two 22bp sequences that are capable of binding and forming a hairpin in a lenti-viral construct. (Adapted from Open Biosystems)

The hairpin that forms activates the cellular drosha/dicer response, resulting in expression arrest for the corresponding transcript (Figure 3). Drosha and dicer process the hairpin shRNAmir to a single strand. The RISC complex binds to the single strand of shRNAmir and the transcript, allowing degradation and silencing of the gene.

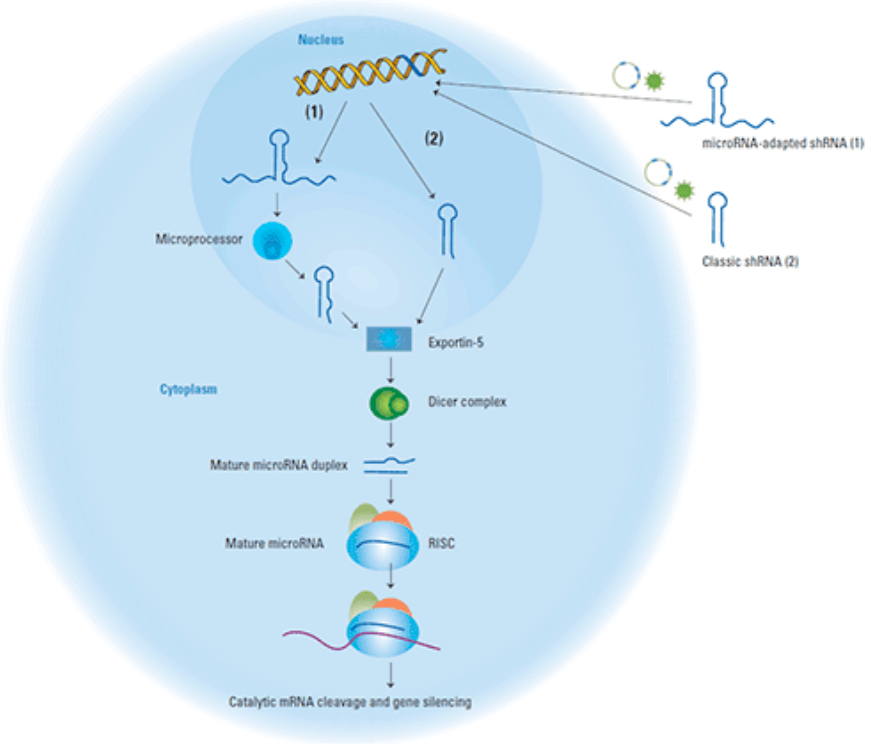

Figure 3: shRNAmir Expression Arrest Mechanism. Cells infected with a single virus containing a shRNAmir construct leads to the expression arrest of a transcript. (Adapted from Open Biosystems)

Function of Smurf2 *In Vivo*

Smurf2 ubiquitous expression has not been studied much; previous *in vivo* studies studied tissue specific expression for osteoblast function. In this project, we use a mouse model to study the consequence of Smurf2 overexpression.

Knockout

Previously, the Smurf2 knockout mouse model was first created by the Zhang group at the National Cancer Institute. This mouse shows genome instability that leads to increased susceptibility to various cancers (Blank et al., 2012). Our lab also generated knockout mice with a different strategy, which have a similar phenotype (in press).

Overexpress

Our lab has created a Smurf2 knock-in mouse using a Cre-LoxP system. A Rosa26-LoxP-STOP-LoxP-Smurf2 mouse was backcrossed to a C57BL/6 background. The Rosa26 is a strong promoter that is capable of ubiquitous expression at the early embryonic stage (Soriano, 1999). The LoxP flanking system allows expression of the gene of interest until repressed with a Cre-LoxP system (Rajewsky et al., 1996). In this case, the STOP is flanked by the LoxP, and represses the expression of Smurf2. To activate the Smurf2 gene, the mice were crossed with Sox2-Cre mice that were able to disrupt the STOP site and allow expression of Smurf2 starting at an early embryonic stage. Figure 4 shows the mechanism that occurs in Smurf2 knock-in mice when crossed with the Sox2-Cre mice.

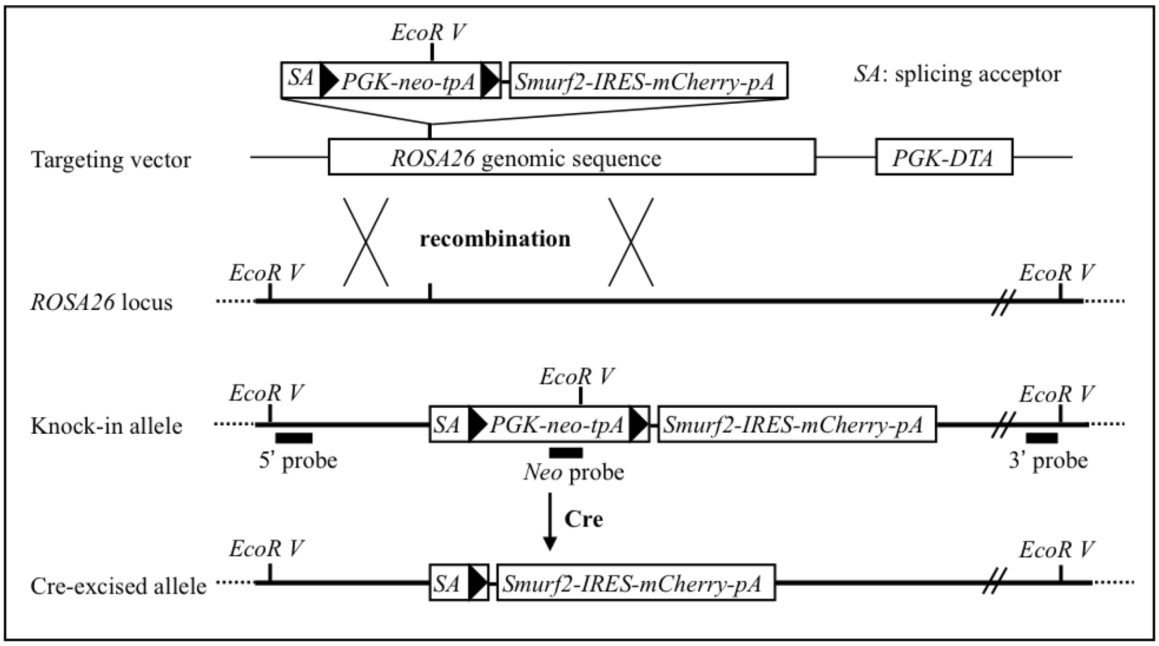

Figure 4: Mechanism of Sox2-Cre-LoxP system in Smurf2 knock-in mice. Smurf2 gene and LoxP-STOP-LoxP insertion into Rosa26 locus inhibits expression of Smurf2. Addition of Sox2-Cre excises STOP and allows expression of Smurf2.

MATERIALS AND METHODS

DNA Cloning

Cloning was used in this project obtain and amplify plasmid constructs needed for DNA transfection. These plasmids included pMD2-VSVG, pCMVdR8.74, dsRED, four different constructs of CDC42BPA, and four different constructs of AHCYL1.

Bacterial Culture

All plasmids were obtained by XL-2 *E. coli* stock containing the construct. The plasmid dsRED was cultured under kanamycin selection; a small amount of bacteria was cultured in 6mL of LB medium containing kanamycin for amplification and collected via miniprep. All other constructs were cultured under ampicillin selection; a small amount of bacteria was streaked out onto ampicillin plates. Single colonies were picked and cultured in 6mL of LB medium containing ampicillin. The CDC42BPA and AHCYL1 plasmids were collected via miniprep. The pMD2-VSVG and pCMVdR8.74 constructs were cultured further in preparation of collection via midiprep.

Plasmid Isolation

Plasmid DNAs in this project were isolated using Quiagen's QIAprep® Spin Miniprep Kit and Quiagen's HiSpeed® Plasmid Purification Kit.

DNA Transfection in 293T

This project required expression of plasmid constructs in cell lines. The DNA was delivered in a lenti-viral construct to integrate their contents into the infected host cell. Viruses packaged were lenti control vector, Notch3, Smurf2 WT, and Smurf2 C716A. Human embryonic kidney 293T cells from culture were plated at a density of 4.5 x 10^6 cells/p100 tissue culture dishes in DMEM medium with 10% fetal bovine serum. Transfection occurred the next day with 2M CaCl2 and 2X HBS at a cell confluence of about 70%.

The DNA was mixed in a 15mL tube; 6.5ug of packaging vector pCMVdR8.74, 3.5ug of envelope vector pMD2-VSVG, 0.2ug of reporter vector dsRED, and 10uL of the DNA of interest. The volume was raised to 437.5uL with 0.1% TE in H_20. The mix was vortexed at a high speed, followed by 62.5uL of CaCl2 and 500uL of HBS, both added drop wise. The final solution was added drop wise onto the 293T cells. Twenty-four hours later, the medium was changed to 9mL of fresh DMEM with 10% FBS. Forty-eight hours post-transfection, the cells were observed under fluorescence microscopy for the presence of dsRED. Supernatants of plates with more than 70% of cells expressing dsRED were collected and stored at -80°C to kill any living cells collected along with the virus.

shRNA Screening

Gene knockdown with shRNA plasmids allowed for identification of possible genes involved in Notch3 induced senescence.

Cell Infection with shRNA Virus and Puromycin Selection

WS1 human fibroblast cells were plated at 1.0 x 10^5 cells/p100. Each p100 plate was infected with 5uL of shRNA library in medium containing 1ug/uL of polybrene. The plates were changed with fresh medium the following day. The shRNA plasmids contain puromycin resistance; two days post infection, medium containing 1ug/mL of puromycin was added. A p60 plate containing WS1 cells as well was used as a selection control; the plate was empty after about 3 days of puromycin exposure. Second round infection occurred after selection.

Cell Infection with Notch3 Virus and BSD Selection

WS1 cells that remained viable after puromycin exposure were then infected with Notch3 virus in medium containing 1ug/uL of polybrene. The plates were changed with fresh medium the following day. The Notch3 plasmid contains BSD resistance; two days post infection , medium containing 1ug/mL of puromycin and 2ug/mL of BSD was added. A p60 containing WS1 cells was again used as a selection control; the plate was empty after 4-5 days of BSD exposure. The cells were kept under puromycin and BSD selection for 12 days, when colonies started forming on the plates.

Isolation of Genomic DNA

Genomic DNA was then isolated from the colonies of the screen using spot trypsinization. Each colony was cultured in an individual well on a 24-well plate

until almost reaching confluence; genomic DNA was isolated using the following protocol. Cells were washed with PBS, and then 200uL of a lysis buffer/5X protease K solution was added. The cells were incubated at 37°C for 2-3 hours, and the supernatant was collected to a 1.5mL Eppendorf tube. Next, 200uL of isopropanol was mixed in and the tube was incubated for 10-15 minutes at room temperature before being spun down for 15 minutes at 14,000 rpm. The supernatant was aspirated and the pellet was washed with 70% ethanol; the tube was spun down again for 7 minutes at 14,000 rpm and then air dried. After the pellet was dry, 50uL of H_20 was added and the tube was left to incubate overnight at 37°C.

Polymerase Chain Reaction

The Genomic DNA extracted from each colony was amplified using Polymerase Chain Reaction and was facilitated with Taq DNA Polymerase purchased from New England Biolabs. The amplified region included the shRNAmir sequence; the amplification product was sent to be sequenced.

Sequencing

The DNA PCR product was purified and sent to Genewiz Inc. for sequencing.

shRNA Conformation

Three shRNAs (PIAS4, AHCYL1, and CDC42BPA) were validated by testing knockdown efficiency and growth curves.

RNA Isolation

RNA was isolated from the cells prior to the secondary infection of Notch3 or Smurf2 to identify the level of knockdown each shRNA induces. RNA was isolated using a Trizol-based protocol, and then run with gel electrophoresis to determine the intergrity of the RNA.

RT-PCR

Invitrogen's Superscript® II Reverse Transcriptase was used to transcribe the extracted RNA into cDNA.

Real-time qPCR

The reverse transcriptase product was run using a Bio-Rad iQ5 machine and software with the aid of SYBR® Green.

Growth Curves

Cells were plated in 6-well plates at around 2 x 10^4 cells/well with two wells for each sample time point. Each set of wells was counted on day 1, 3, 5, and 7 with day 1 being less than 20 hours after cells were plated. A Z1 Coulter® Particle Counter was used to count each sample three times; the average was taken.

Genotyping

Mice were genotyped and marked on the toe at age 7-10 days.

Genomic DNA Extraction

Approximately 2mm of tail was snipped and placed in a PCR tube with 75uL of NaOH and EDTA lysis buffer and incubated at 95°C for 30 minutes and then cooled to 4°C for 15 minutes. Then 75uL of Tris-HCl buffer was added and mixed to neutralize the solution.

Polymerase Chain Reaction

The extracted genomic DNA was amplified using Polymerase Chain Reaction using primers that surrounded the region of interest, Smurf2 WT, Smurf2 C716A, or Cre. Amplification was aided by Lambda Biotech's Taq Polymerase. The PCR product was run on a 1% agarose gel with gel electrophoresis to determine the genotypes.

OBSERVATION OF CONSEQUENCE OF SMURF2 *IN VIVO*

Observation of the Smurf2 overexpressed mice was carried out by a bi-weekly and weekly record of weight as well as determination of gene expression by Western and real-time PCR.

Growth Curve

Growth was measured from shortly after birth until death. Weight was measured in grams by placing the mouse in a beaker that was zeroed on a balance.

Organ Extraction: RNA and Lysate Extraction

Eight organs; liver, heart, lung, kidney, pancreas, spleen, colon, and skin were harvested and weighed. Each organ was frozen in liquid nitrogen and crushed into powder for subsequent use for lysate and RNA extraction.

RNA was extracted from the spleen using the above mentioned Trizol based procedure. The RNA was reverse-transcribed and analyzed with real-time PCR. Lysate was extracted from all the organs using RIPA buffer with 20X protease inhibitor. Concentration was measured at 562 nanometers. Lysates were run on a Western blot and probed for Smurf2, p21, p16, and tubulin.

Bone Marrow Extraction

The entire bone marrow extraction process was performed on ice. Mice were double-killed using Isoflurane and cervical dislocation. Hind limbs were severed at hip joint and forelimbs at the shoulder joint. Limbs were placed in a p60 plate containing a staining (Biotin-, Flavin-, Pheno-red deficient RPMI1640) medium. Skin and muscle was scraped away to the bone with a razor blade and the knee and elbow joints were disarticulated to harvest the femur, tibia, and humorous bones. The ends of the bones were cut to expose the marrow cavities; bones were completely flushed with staining solution using a 5mL syringe and a 25G needle. An 18G needle is subsequently used to break the large chunks of marrow into small pieces. Cells are filtered with a 70um nylon mesh into a 15uL tube and the final volume of cells is brought up to 10mL with the staining solution.

A 10X dilution of cells is counted using a hemocytometer. The bone marrow was extracted for RNA using the method mentioned above in prep for rtPCR.

RESULTS

Production of Smurf2 and Notch3 Viruses

HEK-293T cells were used to package the viruses used in this project via transfection. A plasmid expressing a red fluorescent protein dsRED was used in transfection to determine the efficiency of the transfections; Figure 5 shows representative images of 293T cells after transfection. Stronger dsRED fluorescence correlates with a better efficiency; efficiencies lower that 80% were not used.

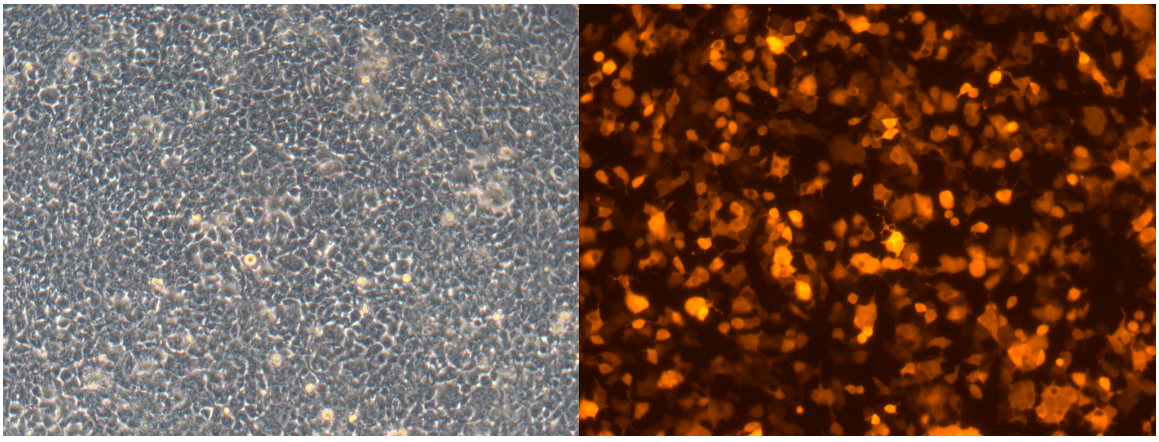

Figure 5: HEK-293T Transfection Efficiency. Transfection efficiency is shown by dsRED fluorescence: regular light (left) and green fluorescent light (right) shows the usual percentage of HEK-239T infected by the virus.

shRNA Screen for Genes Involved in Notch3-Induced Senescence

Our lab had previously screened several candidates using Smurf2, so I concentrated on screening with Notch3. Seven genes were identified from the Notch3 screen; Table 1 shows the genes identified along with the chromosome location and the sense shRNA sequence. CDC42 binding protein kinase alpha (CDC41BPA) is highlighted in the table; this gene was studied further in attempt to confirm that it operates downstream of Notch3. Between the previous Smurf2

screening and the current Notch3 screen, five genes were analyzed further: SUMO2, Catalase, PIAS4, AHCYL1, and CDC42BPA.

Pool #	Gene Name	Identity Match	Chromosome Location	Sense shRNA sequence 5' -> 3'
8	Inter-genic region	21/22	8	CCGTCTCCAGACATTTAAAGAT
9	Inter-genic region	21/22	1	CTGAAGATGTACTGGAACTAAA
9	Glutamate receptor, ionotropic, kainite 3	21/22	1p34-p33	CCCTTGGTTTCTCCTATGAGAT
10	**CDC42 binding protein kinase alpha**	**21/22**	**1q42.11**	**CAAGCTGGAAGTTCATACAGAA**
11	Transcription factor AP-2 beta	21/22	6p12	ACCTCCCTTCCTCACATTGTTA
13	Inter-genic region	21/22	14	AGCATGTCACTTGTTCTGTTAA
13	Inter-genic region	21/22	20	AGCCTTAAGTTCCACCACACTA

Table1: Seven Candidate Genes That May Act Downstream of Notch 3. A summary of the sequencing data obtained from the Notch3 screening. The shRNA targeted genes are shown, as well as the nucleotide match between the gene and siRNA and chromosome location. CDC42 binding protein kinase alpha was chosen to research further as a possible candidate.

Test of Knockdown of Candidate Genes

Total RNA was extracted from cells infected with lenti-virus expressing shRNA targeting SUMO2, Catalase, PIAS4, AHCYL1, and CDC42BPA. After reverse transcription, RT-qPCR was used to determine if the shRNAs were able to induce a sufficient knockdown in the cells.

SUMO2 and CATALASE shRNA was unable to produce an adequate knockdown (data not shown), so confirmation of these genes was discontinued.

Both shRNAs tested induced more than 50% knockdown of PIAS4 in WS1 fibroblast cells (Figure 6) when infected with 200uL of shRNA lenti-virus.

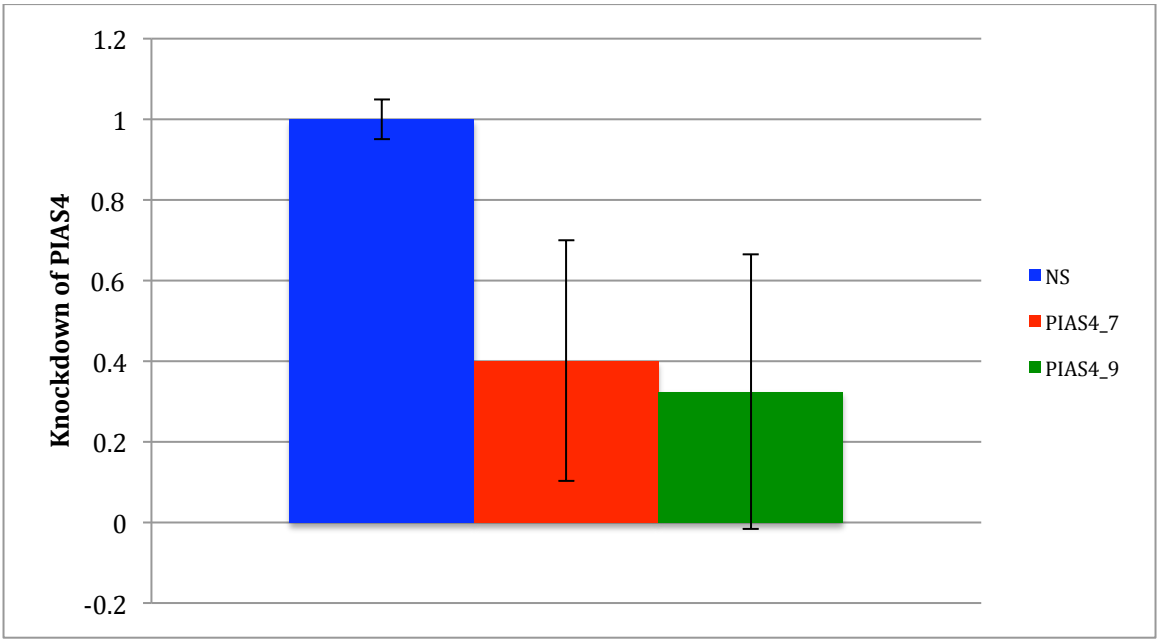

Figure 6: PIAS4_7 and PIAS4_9 shRNAs Produce a More Than Fifty Percent Knockdown in WS1 cells. RNA was collected from WS1 cells and reverse transcribed to cDNA for real time PCR from WS1 cells transfected with 200uL non-silencing shRNA (blue), PIAS4_7 (red), and PIAS4_9 (green). Non-silencing shRNA was normalized to 1.

Four different shRNAs were tested for AHCYL1, giving various knockdowns for a 100uL virus infection in WS1 fibroblast cells (data not shown). The best shRNA were retested in LF1 cells with 250uL of virus, giving more than an 80% knockdown (Figure 7).

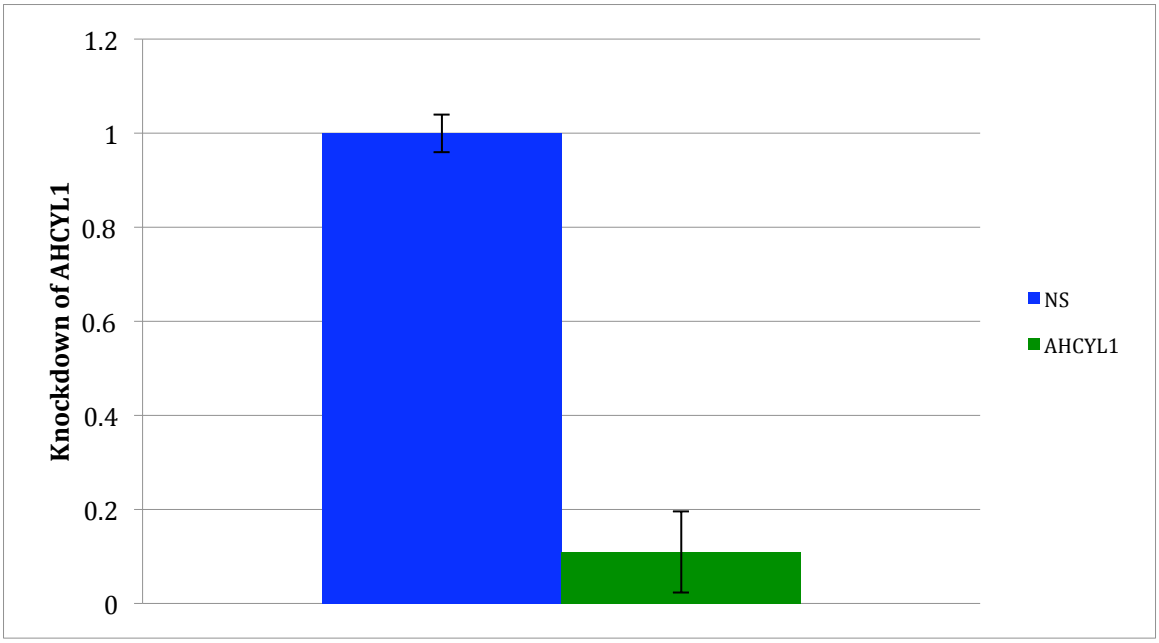

Figure 7: AHCYL1_4 shRNA Produces a More Than Eighty Percent Knockdown in LF1 cells. RNA was collected from LF1 cells and reverse transcribed to cDNA for real time PCR from LF1 cells transfected with 250uL of non-silencing shRNA (blue) and AHCYL1_4 (green). Non-silencing shRNA was normalized to 1.

Four different shRNAs were also tested for CDC42BPA; these also gave various knockdowns for a 100uL virus infection in WS1 fibroblast cells (data not shown). The best two shRNAs were retested in LF1 cells with 250uL of virus, giving more than a 40% knockdown (Figure 8).

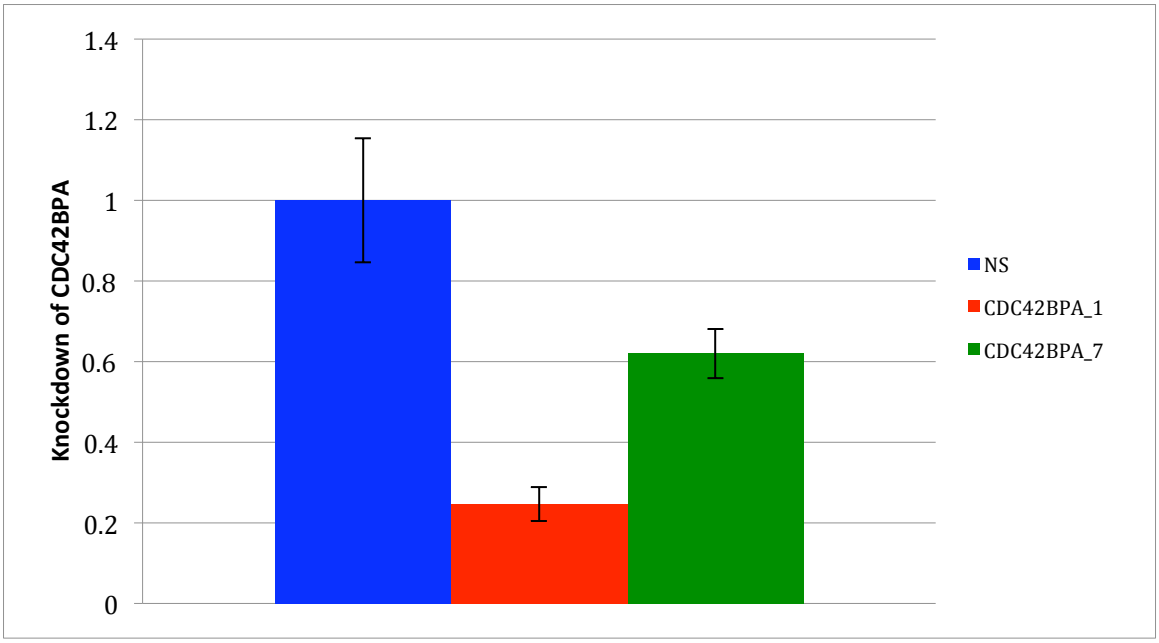

Figure 8: CDC42BPA (1,7) shRNA Produce a More Than Forty Percent Knockdown in LF1 cells. RNA was collected from LF1 cells and reverse transcribed to cDNA for real time PCR from WS1 cells transfected with 250uL of non-silencing shRNA (blue), CDC42BPA_1 (red), and CDC42BPA_7 (green). Non-silencing shRNA was normalized to 1.

Validation of PIAS4, AHCYL1, and CDC42BPA

In order to ensure that the candidates that were screened were not background, growth curves were used. WS1 or LF1 fibroblast cells with non-silencing, PIAS4, AHCYL1, and CDC42BPA shRNA were infected with lenti-virus control vector and either Smurf2 WT as well as Smurf2 C716A or Notch3 challenge viruses. The cells were plated four days post-infection (Notch3) or five days post-infection (Smurf2 WT and C716A).

Figure 9 below shows the growth curve data from PIAS4_7 and non-silencing knockdown cells with a lenti-virus control vector, Smurf2 WT, or Smurf2 C716A challenge in WS1 cells. The data shows that PIAS4/lenti control growth rate is about the same as non-silencing/lenti control. The data also shows that PIAS4 knockdown (dashed blue and red), when challenged with Smurf2 WT and Smurf2 C716A, does

not lead to a significant rescue of senescence when compared to non-silencing knockdown (solid blue and red).

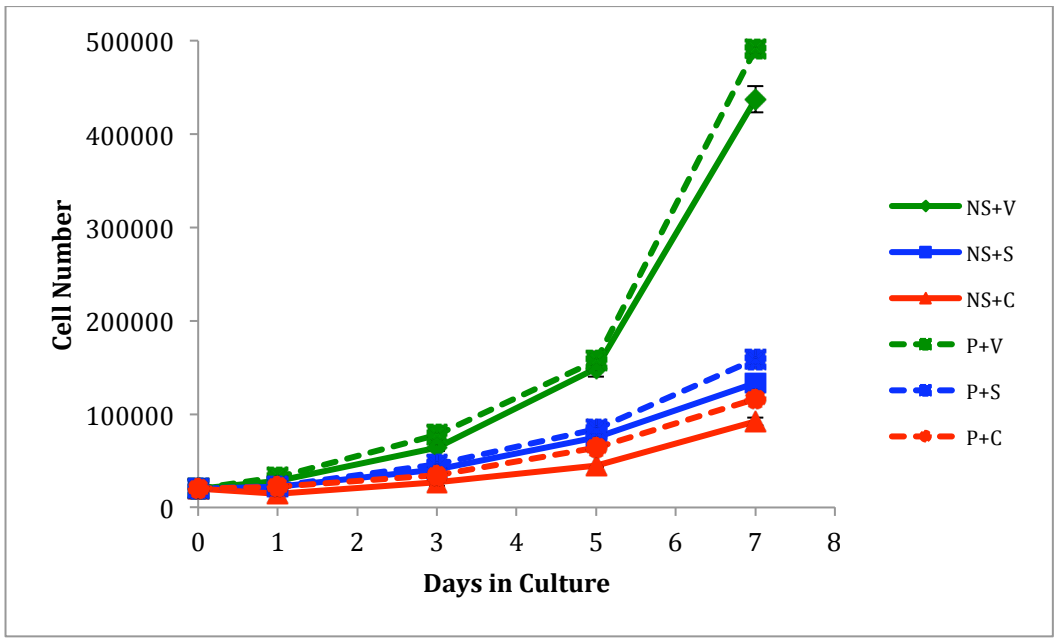

Figure 9: PIAS4_7 Knockdown Does Not Lead to Significant Rescue of Smurf2 WT and Smurf2 C716A Induced Senescence. Cell growth data was collected from LF1 cells transfected with non-silencing shRNA/lenti-virus control vector (solid green), non-silencing shRNA/Smurf2 WT (solid blue), non-silencing/Smurf2 C716A (solid red), PIAS4/lenti-virus control vector (dashed green), PIAS4/Smurf2 WT (dashed blue), and PIAS4/Smurf2 C716A (dashed red). Data shows that PIAS4 cells challenged with either Smurf2 WT or Smurf2 C716A are not rescued from the control senescence phenotype shown by non-silencing shRNA/Smurf2 WT and non-silencing shRNA/Smurf2 C716A.

Figure 10 below shows the growth curve data from AHCYL1 and non-silencing knockdown cells with a lenti-virus control vector, Smurf2 WT, or Smurf2 C716A challenge in LF11 cells. The data shows that AHCYL1/lenti control growth rate is slower than non-silencing/lenti control. The data also shows that AHCYL1 knockdown (dashed blue and red), when challenged with Smurf2 WT and Smurf2 C716A, does not lead to a significant rescue of senescence when compared to non-silencing knockdown (solid blue and red).

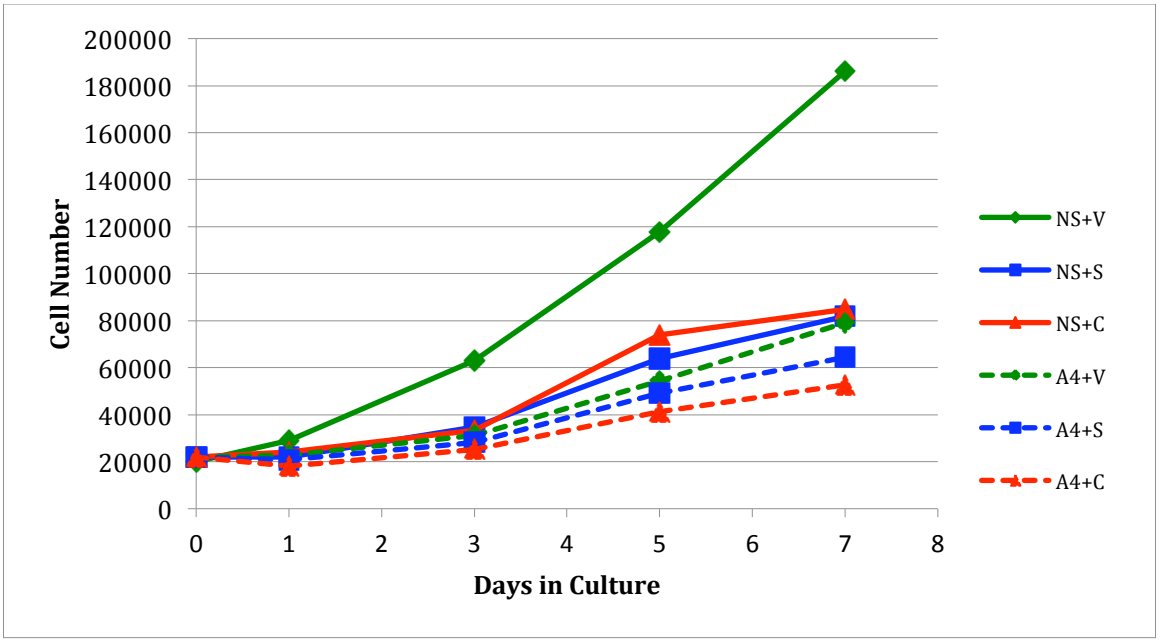

Figure 10: AHCYL1 Knockdown Does Not Lead to Significant Rescue of Smurf2 WT and Smurf2 C716A Induced Senescence. Cell growth data was collected from LF1 cells transfected with non-silencing shRNA/lenti-virus control vector (solid green), non-silencing shRNA/Smurf2 WT (solid blue), non-silencing/Smurf2 C716A (solid red), AHCYL1/lenti-virus control vector (dashed green), AHCYL1/Smurf2 WT (dashed blue), and AHCYL1/Smurf2 C716A (dashed red). Data shows that AHCYL1 cells challenged with either Smurf2 WT or Smurf2 C716A are not rescued from the control senescence phenotype shown by non-silencing shRNA/Smurf2 WT and non-silencing shRNA/Smurf2 C716A.

Figure 11 below shows the growth curve data from CDC42BPA_1 and non-silencing knockdown cells with a lenti-virus control vector or Notch3 challenge in LF1 cells. The data shows that CDC42BPA/lenti control growth rate is faster than non-silencing/lenti control. The data also shows that CDC42BPA knockdown (dashed blue), when challenged with Notch3, does not lead to a significant rescue of senescence when compared to non-silencing knockdown (solid blue).

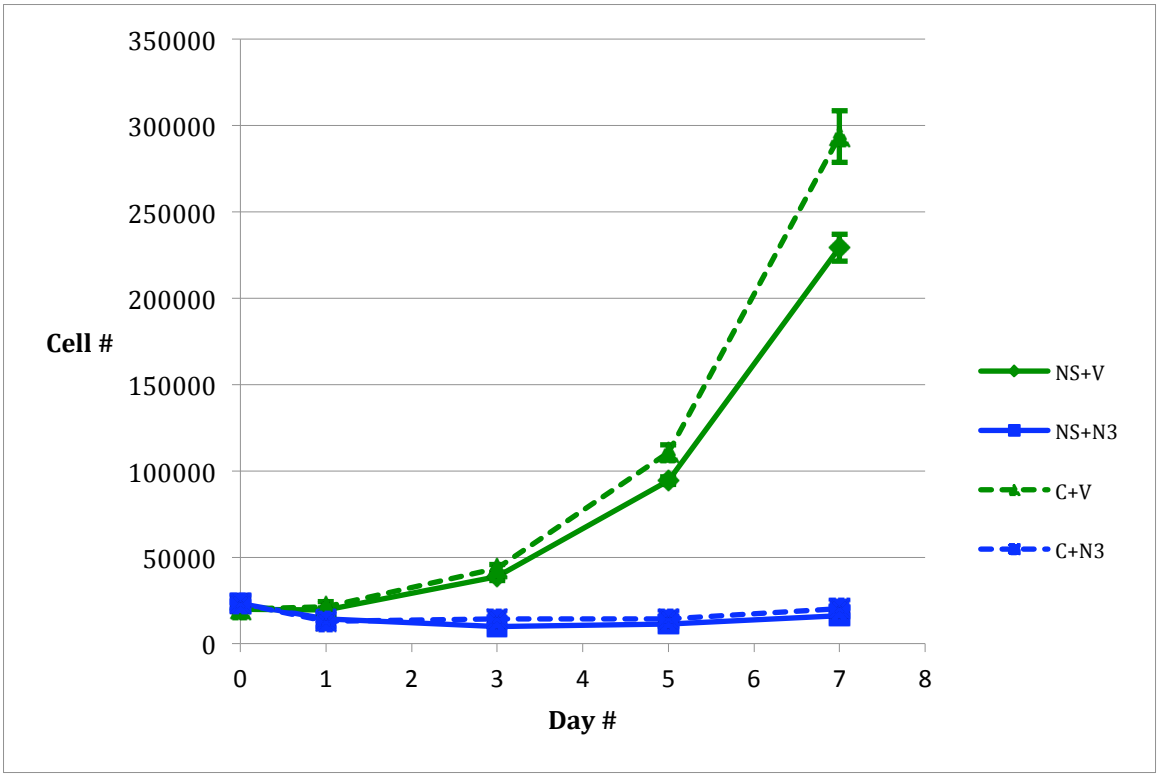

Figure 11: CDC42BPA_1 Knockdown Does Not Lead to Significant Rescue of Notch3 Induced Senescence. Cell growth data was collected from LF1 cells transfected with non-silencing shRNA/lenti (solid green), non-silencing shRNA/Notch3 (solid blue), CDC42BPA/lenti (dashed green), and CDC42BPA/Notch3 (dashed blue). Data shows that CDC42BPA cells challenged with Notch3 are not rescued from the control senescence phenotype shown by non-silencing shRNA/Notch3.

Figure 12 below shows the growth curve data from CDC42BPA_7 and non-silencing knockdown cells with a lenti-virus control vector, Smurf2 WT, or Smurf2 C716A challenge in LF11 cells. The data shows that CDC42BPA/lenti control growth rate is slower than non-silencing/lenti control. The data also shows that CDC42BPA knockdown (dashed blue and red), when challenged with Smurf2 WT and Smurf2 C716A, does lead to a significant rescue of senescence when compared to non-silencing knockdown (solid blue and red).

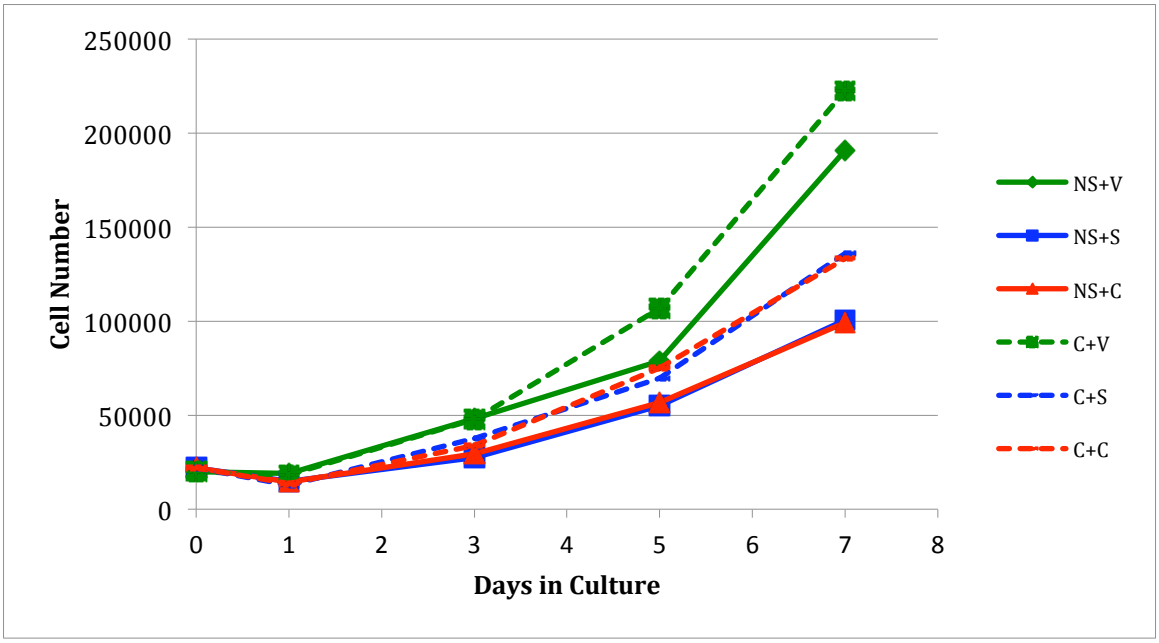

Figure 12: CDC42BPA_7 Knockdown Does Lead to Significant Rescue of Smurf2 WT and Smurf2 C716A Induced Senescence. Cell growth data was collected from LF1 cells transfected with non-silencing shRNA/lenti-virus control vector (solid green), non-silencing shRNA/Smurf2 WT (solid blue), non-silencing/Smurf2 C716A (solid red), CDC42BPA/lenti-virus control vector (dashed green), CDC42BPA/Smurf2 WT (dashed blue), and CDC42BPA/Smurf2 C716A (dashed red). Data shows that CDC42BPA cells challenged with either Smurf2 WT or Smurf2 C716A are rescued from the control senescence phenotype shown by non-silencing shRNA/Smurf2 WT and non-silencing shRNA/Smurf2 C716A.

Senescence Regulation by Smurf2 *In Vivo*

To analyze what happens when Smurf2 is overexpressed in mice, we weighed the mice every one to two weeks and checked Smurf2, p21, and p16 expression levels in organs and bone marrow.

There were seven mice in the litter: three were Sox2-Cre and four were Sox2-Cre/Smurf2. For the first month, the mice were weight every other week; they were weighed every week for the second month (Figure 13). The data shows that the Sox2-Cre/Smurf2 (blue) mice weigh less than the Sox2-Cre (red) mice for approximately the first forty days.

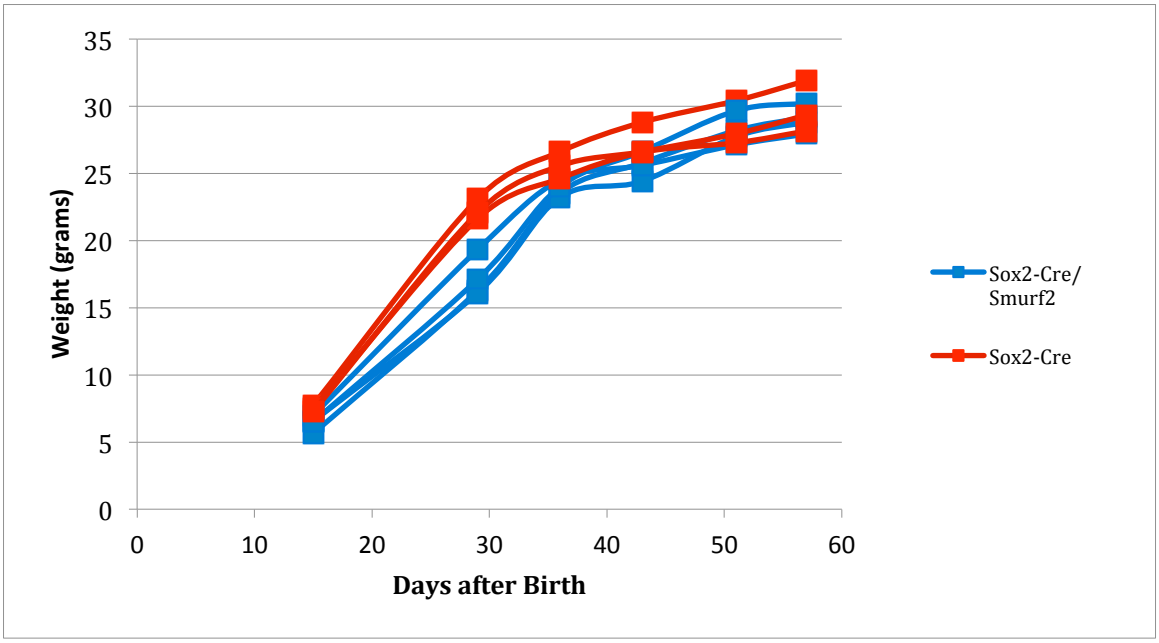

Figure 13: Smurf2 Overexpressing Mice Weight Less. Mice were weighed every two weeks and then every week for two months. The litter was seven mice: three were Sox2-Cre (red) and four were Sox2-Cre/Smurf2 (blue).

To determine protein expression, lysate was extracted from eight organs and run on a Western blot. The organs extracted were liver, kidney, spleen, pancreas, colon, lung, heart, and skin. The membrane was probed with three antibodies: Smurf2, p21, and p16, but p21 and p16 were undetected. As seen with Figure 14, Smurf2 protein is overexpressed in Sox2-Cre/Smurf2 mice when compared to Sox2-Cre mice.

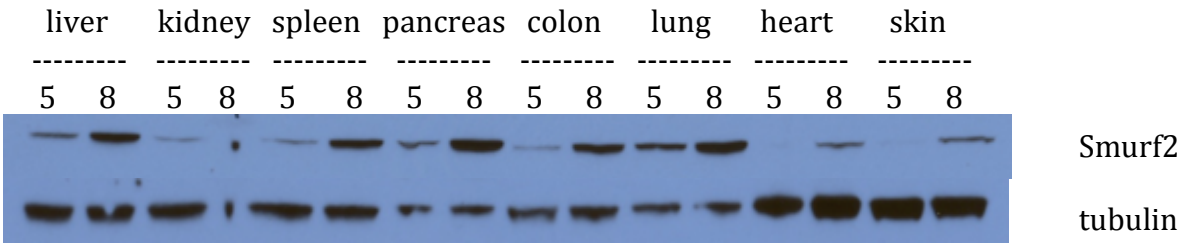

Figure 14: Smurf2 Protein is Overexpressed in Sox2-Cre/Smurf2 Mice.
Western blot of Sox2-Cre mouse #5 and Sox2-Cre/Smurf2 mouse #8 organs. Organs include liver, kidney, spleen, pancreas, colon, lung, heart, and skin. Membrane was probed with Smurf2.

The gene expression of Smurf2, p21, and p16 was determined using an assay more sensitive than a Western blot. RNA was extracted from spleen and analyzed using real-time PCR. As seen in Figure 15, Smurf2 and p21 RNA is overexpressed in Sox2-Cre/Smurf2 (blue) mice when compared to Sox-Cre (red) mice. The data also shows that p16 is not overexpressed in Sox2-Cre/Smurf2 mice.

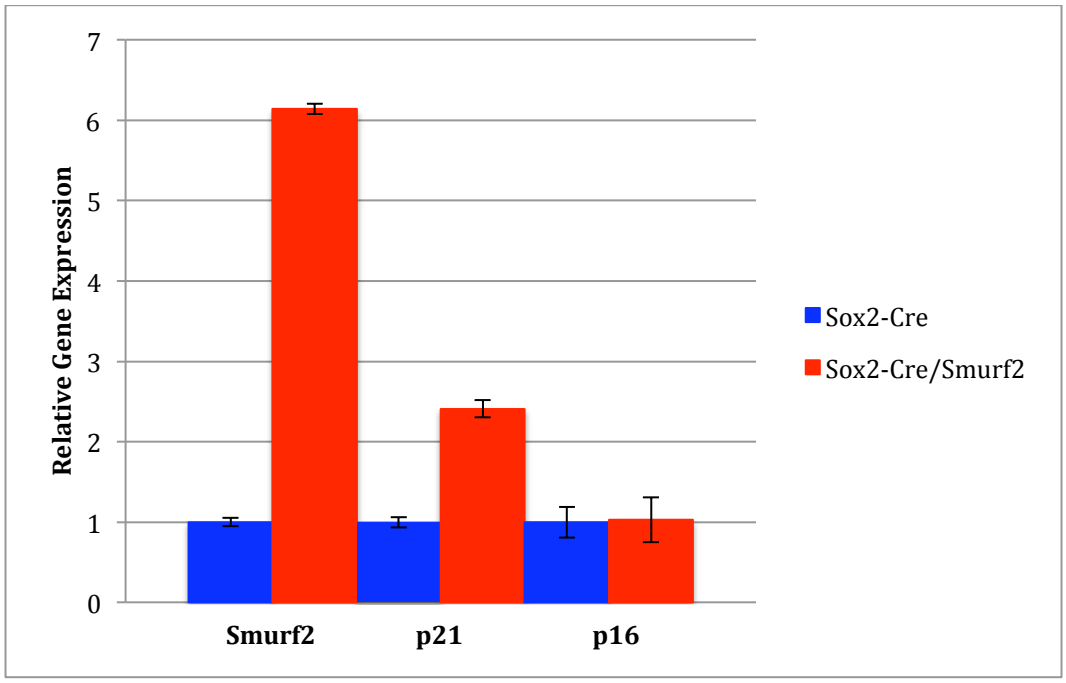

Figure 15: Smurf2 and p21 RNA is Overexpressed in Sox2-Cre/Smurf2 mice. RNA was extracted from spleen in Sox2-Cre (blue) and Sox2-Cre/Smurf2 (red) mice. Expression of Smurf2, p21, and p16 was analyzed. Sox2-Cre gene expression was normalized to 1.

The gene expression of Smurf2, p21, and p16 RNA was also determined with bone marrow and analyzed using real-time PCR. As seen in Figure 16, Smurf2 RNA is overexpressed in Sox2-Cre/Smurf2 (blue) mice when compared to Sox-Cre (red) mice. The data also shows that p21 is not significantly overexpressed in Sox2-Cre/Smurf2 mice and that p16 expression is undetectable.

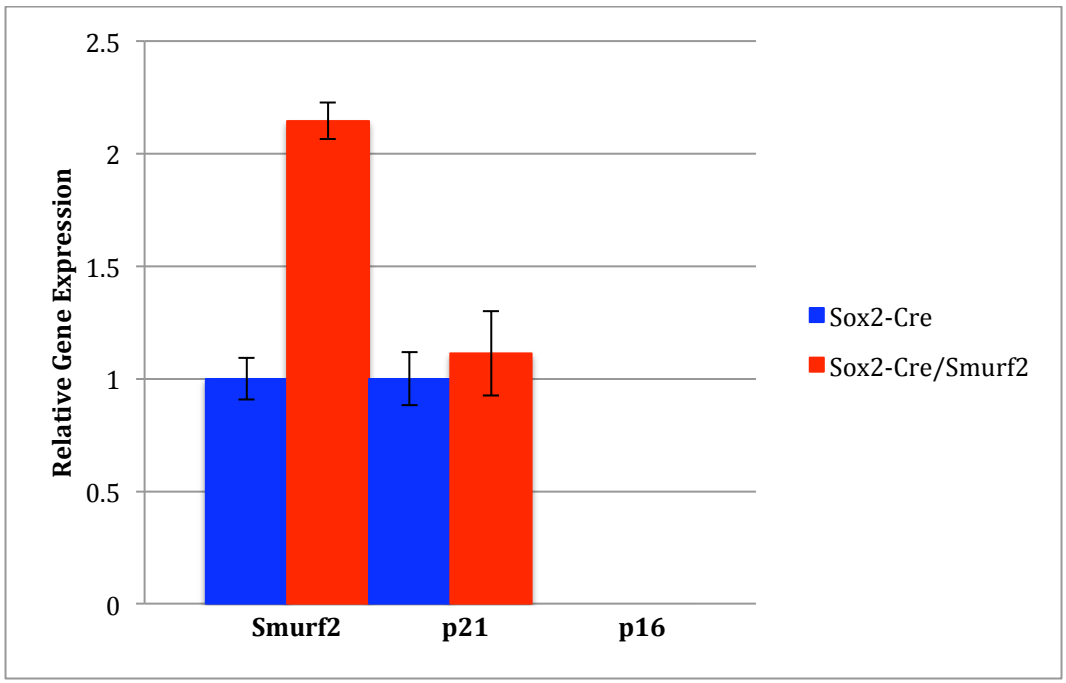

Figure 16: Smurf2 RNA is Overexpressed in Sox2-Cre/Smurf2 mice. RNA was extracted from bone marrow in Sox2-Cre (blue) and Sox2-Cre/Smurf2 (red) mice. Expression of Smurf2, p21, and p16 was analyzed. Sox2-Cre gene expression was normalized to 1.

DISCUSSION

Discussion

This project was successful in using shRNAmir gene knockdown screening to identify potential genes downstream of Notch3. Seven candidate genes were identified from this screening process, one of which was further investigated with five genes in the Smurf2 senescence pathway. My data suggests that knockdown of CDC42BPA allows partial escape of Smurf2 induced senescence, while knockdown of CDC42BPA does not allow significant rescue from Notch3-induced senescence and knockdown of PIAS4 and AHCYL1 does not allow significant rescue from Smurf2-induced senescence.

This project was also successful in determining preliminary characterization of the function of Smurf2 in senescence regulation *in vivo*. Smurf2 overexpression is able to impact growth and regulate p21 in young mice.

PIAS4, AHCYL1, and CDC42BPA

PIAS4, AHCLY1, and CDC42BPA were identified as candidate genes whose down-regulation allows the escape of Smurf2- or Notch3-induced senescence in WS1 and LF1 cells.

PIAS4

It has been suggested previously that PIAS4 is involved in senescence (Rytinki et al., 2009). PIAS, or protein inhibitors of activated STATs, is able to inhibit STAT as its name suggests (Desrivières et al., 1996). As STAT activates transcription,

PIAS is able to inhibit transcription (Desrivières et al., 1996). PIAS4 (PIASy or gamma) is shown to act as a SUMO-E3 ligase for Smad3 and p53 (Imoto et al., 2003).

My results indicate that knockdown of PIAS4 is not sufficient to allow fibroblasts to escape Smurf2-induced senescence. It is possible that the level of knockdown in my experiments was not depleted enough to interfere with the function of PIAS4, or that other PIAS proteins (PIAS1-3) compensate for the knockdown of PIAS4. In the case of compensation, a function interference of PIAS activity would be more suitable in the test of their function in Smurf2-induced senescence. It is also possible that knockdown of PIAS4 only compromises only one of the senescence pathways, which is not sufficient for a full escape of Smurf2-induced senescence. It will be interesting to investigate if PIAS4 collaborates with other genes in regulating Smurf2-induced senescence.

AHCYL1

It is known that AHCYL can regulate both senescence pathways through p53 and p16 (Leal et al., 2008). AHCYL1, or s-adenosylhomocysteine hydrolase-like 1, is involved in the hydrolysis of S-adenosyl-L-homocysteine to L-homocysteine and adenosine (Leal et al., 2008). Although there is little research on AHCYL1 in particular, inactivation of AHCYL in general induced cell resistance to p53 and p16-induced replicative arrest (Leal et al., 2008). AHCYL has also been shown to inhibit p53 transcriptional activity and DNA damage-induced transcription of p21 (Leal et al., 2008).

My data gives evidence that knockdown of AHCYL1 is not sufficient to resuce fibroblasts from Smurf2-induced senescence. As very good knockdown of AHCYL1 was achieved, it is likely that the level of AHCYL1 knockdown interfered with its function. A possibility is that AHCYL2 was able to compensate for the knockdown of AHCYL1, so again, a function interference of AHCYL activity might be more suitable in testing its function. An alternative reason is that AHCYL1 knockdown causes the WS1 and LF1 fibroblast cells to grow very slowly, even without the secondary infection; faster growth was unable to be achieved. So although AHCYL1 knockdown with Smurf2 WT and Smurf2 C716A challenge grew similarly to AHCYL1 knockdown with lenti-virus control vector, all three grew similarly to non-silencing knockdown with Smurf2 WT and Smurf2 C716A challenge.

CDC42BPA

CDC42BPA is known to regulate p53 is the senescence pathway (Sirotkin et al., 2008). CDC42BPA (CDC42 binding protein kinase alpha) knockdown is shown to inhibit the expression of p53 and PCNA, or proliferating cell nuclear antigen in ovarian cells (Sirotkin et al., 2008). PCNA promotes DNA synthesis during S phase and provides protection from apoptosis during G1 phase (Sirotkin et al., 2008).

My results indicate that knockdown of CDC42BPA is not sufficient to allow fibroblasts to escape Notch3-induced senescence; however, the knockdown was sufficient to partially rescue cells from Smurf2-induced senescence. It is possible that the knockdown level of CDC42BPA in my experiments, while sufficient to interfere with its function while downstream of Smurf2, was not low enough to

interfere with the function of CDC42BPA when downstream of Notch3. Because CDC42BPA is only shown to interact with one of the senescence pathways, this may not be sufficient for escape of Notch3-induced senescence. It will be interesting to further determine the interaction of Smurf2 with CDC42BPA, as well as the interaction of CDC42BPA with other genes in the senescence pathway. This research may be able to enlighten us on if and how CDC42BPA interacts with Notch3.

Smurf2 *In Vivo*

Smurf2 overexpression was able to affect growth in young mice for a short period of time. However, the mice seemed to have compensated for this abnormal development, as this stunted growth lasted for less than two months. Smurf2 overexpression in young mice seemed to adhere to a similar senescence pathway that occurs *in vitro*. Smurf2 was shown to regulate p21, which is consistent with *in vitro* data. However, as p16 did not seem to be regulated by Smurf2, this could have occurred due to the young age of the mice. p16 has been seen to be vastly increased during senescence (Alcorta, et al., 1996), indicating that p16 will most likely not become present in mice until an older age.

Growth rates of Smurf2 overexpressed mice should be repeated, possibly with weights being measured at more frequent intervals. Gene expression should also be determined at additional ages to determine if the expression changes as the mice age. Our lab also contains Smurf2 C716A mice, it will be interesting to see if overexpression of Smurf2 C716A gives similar consequences as Smurf2 WT overexpression.

REFERENCES

Alcorta DA, Xiong Y, Phelps D, Hannon G, Beach D, Barrett JC. 1996. Involvement of the cyclin-dependent kinase inhibitor p16 (INK4a) in replicative senescence of normal human fibroblasts. PNAS 93(24): 13742-13747.

Allenspach EJ, Maillard I, Aster JC, Pear WS. 2002. Notch Signaling in Cancer. Cancer Biology & Therapy 1(5): 466-476.

Bayreuther K, Rodemann HP, Hommel R, Dittmann K, Albiez M, Francz PI. 1988. Human skin fibroblasts *in vitro* differentiate along a terminal cell lineage. PNAS 85: 5112-5116.

Beauséjour CM, Krtolica A, Galimi F, Narita M, Lowe SW, Yaswen P, Campisi J. 2003. Reversal of human cellular senescence: roles of the p53 and p16 pathways. EMBO Journal 22(16): 4212-4222.

Benanti JA, Galloway DA. 2004. Normal Human Fibroblasts Are Resistant to RAS-Induced Senescence. Molecular and Cellular Biology 24(7): 2842-2852.

Blank M, Tang Y, Yamashita M, Burkett SS, Cheng SY, Zhang YE. 2012. A tumor suppressor function of Smurf2 associated with controlling chromatin landscape and genome stability through RNF20. Nature Medicine 18(2): 227-234.

Desrivières, S, Kunz C, Barash I, Vafaizadeh V, Borghouts C, Groner B. 2006. The Biological Functions of the Versatile Transcription Factors STAT3 and STAT5 and New Strategies for their Targeted Inhibition. Journal of Mammary Gland Biology and Neoplasia 11(1): 75-87.

Dimri GP, Lee X, Basile G, Acosta M, Scott G, Roskelley C, Medrano EE, Linskens M, Rubeli I, Pereira-Smith O, Peacocke M, Campisi J. 1995. A biomarker that identifies senescent human cells inculture and in aging skin *in vivo*. PNAS 92: 9363-9367.

Giovannini C, Gramantieri L, Chieco P, Minguzzi M, Lago F, Pianetti S, Ramazzotti E, Marcu KB, Bolondi L. 2009. Selective ablation of Notch3 in HCC enhances doxorubicin's death promoting effect by a p53 dependent mechanism. Journal of Hepatology 50(5): 969-979.

Harley CB, Futcher AB, Greider CW. 1990. Telomeres shorten during ageing of human fibroblasts. Nature 345: 458-460.

Hayflick L, Moorhead PS. 1961. The serial cultivation of human diploid cell strains. Experimental Cell Research 25: 585–621.

Herbig U, Jobling WA, Chen BPC, Chen DJ, Sedivy JM. 2004. Telomere Shortening Triggers Senescence of Human Cells through a Pathway Involving ATM, p53, and $p21^{CIP1}$, but Not $p16^{INK4a}$. Molecular Cell 14: 501–513.

Herbig U, Wenyi W, Dutriaux A, Jobling WA, Sedivy JM. 2003. Real-time imaging of transcriptional activation in live cells reveals rapid up-regulation of the cyclin-dependent kinase inhibitor gene CDKN1A in replicative cellular senescence. Aging Cell 2(6): 295-304.

Hütter E, Unterluggauer H, Überall F, Schramek H, Jansen-Dürr P. 2002. Replicative senescence of human fibroblasts: the role of Ras-dependent signaling and oxidative stress. Experimental Gerontology 37(10-11): 1165-1174.

Imoto S, Sugiyama K, Muromoto R, Sato N, Yamamoto T, Matsuda T. 2003. Regulation of Transforming Growth Factor-β Signaling by Protein Inhibitor of Activated STAT, PIASy through Smad3. Journal of Biological Chemistry 278:34253-34258.

Kim NW, Piatyszek MA, Prowse KR, Harley CB, West MD, Ho PLC, Coviello GM, Wright WE, Weinrich SL, Shay JW. 1994. Specific association of human telomerase activity with immortal cells and cancer. Science 266: 2011-2016.

Kong Y, Cui H, Zhang H. 2011. Smurf2-mediated ubiquitination and degradation of Id1 regulates p16 expression during senescence. Aging Cell 10(6): 1038-1046.

Leal JF, Ferrer I, Blanco-Aparicio C, Hernández-Losa J, Ramón y Cajal S, Carnero A, LLeonart ME. 2008. *S-adenosylhomocysteine hydrolase* downregulation contributes to tumorigenesis. Carcinogenesis 29(11): 2089-2095.

Lin X, Liang M, Feng XH. 2000. Smurf2 Is a Ubiquitin E3 Ligase Mediating Proteasome-dependent Degradation of Smad2 in Transforming Growth Factor-β Signaling. Journal of Biological Chemistry 275(47): 36818-36822.

Oyama T, Harigaya K, Muradil A, Hozumi K, Habu S, Oguro H, Iwama A, Matsuno K, Sakamoto R, Sato M, Yoshida N, Kitagawa M. 2007. Mastermind-1 is required for Notch signal-dependent steps in lymphocyte development *in vivo*. PNAS 104(23): 9764-9769.

Rajewsky K, Gu H, Kühn R, Betz UAK, Müller W, Roes J, Schwenk F. 1996. Conditional Gene Targeting. Journal of Clinical Investigation 98(3) 600-603.

Ruas M, Peters G. 1998. The $p16^{INK4a}$/CDKN2A tumor suppressor and its relatives. Biochimica et Biophysica Acta 21378(2): F115-F177.

Rytinki M, Kaikkonen S, Pehkonen P, Jääskeläinen T, Palvimo J. PIAS proteins: pleiotropic interactors associated with SUMO. Cellular and Molecular Life Sciences 66: 3029-3041.

Sirotkin AV, Ovcharenko D, Benčo A, Mlynček M. 2008. Protein kinases controlling PCNA and p53 expression in human ovarian cells. Functional & Integrative Genomics 9:185-195.

Sherwood SW, Rush D, Ellsworth JL, Schimke RT. 1988. Defining cellular senescence in IMR-90 cells: A flow cytometric analysis. Proc Natl Acad Sci USA 85: 9086–9090.

Soriano P. 1999. Generalized lacZ expression with the ROSA26 Cre reporter strain. Nature Genetics 21: 70-71.

Vaziri H, West M, Allsop RC, Davison TS, Wu Y, Arrowsmith CH, Poirier GG, Benchimol S. 1997. ATM-dependent telomere loss in aging human diploid fibroblasts and DNA damage lead to the post-translational activation of p53 protein involving poly(ADP-ribose) polymerase. EMBO Journal 16(19): 6018-6033.

Zhang H. 2007. Molecular signaling and genetic pathways of senescence: Its role in tumorigenesis and aging. Journal of Cellular Physiology 210(3): 567-574.

Zhang H, Cohen SN. 2004. Smurf2 up-regulation activates telomere-dependent senescence. Genes & Development 18**:** 3028-3040.

Zhang H, Teng Y, Kong Y, Kowalski PE, Cohen SN. 2008. Suppression of human tumor cell proliferation by Smurf2-induced senescence. Journal of Cellular Physiology 215(3): 613-620.

Zheng W, Wang H, Xue L, Zhang Z, Tong T. 2004. Regulation of cellular senescence and p16(INK4a) expression by Id1 and E47 proteins in human diploid fibroblast. Journal of Biological Chemistry 279(30) 31524-31532.